**ANDRAWES, K. Z. and McGOWN, A.**
University of Strathclyde, Glasglow, U.K.
**WILSON-FAHMY, R. F.**
University of Cairo, Egypt
**MASHHOUR, M. M.**
University of Zagazig, Egypt

# The Finite Element Method of Analysis Applied to Soil-Geotextile Systems

# La méthode d'element fini d'analyse appliqué aux systèmes de sol géotextiles

The paper describes the nature of the elements used to represent soil-geotextile systems for the purpose of predicting their stress-strain behaviour. The stiffness matrices used to characterise each of these are given and the stress-strain laws adopted to represent the material properties are detailed. A finite element mesh so derived is then applied to the prediction of the behaviour of a footing resting on dense sand with or without a single layer of geotextile placed at different depths in various tests. It is shown that if the soil properties can be correctly represented in the soil elements, good correlations between predicted and measured data is obtained up to about 85 per cent of peak load. Beyond this, the finite element method is inappropriate as local failures in the soil occur which cannot be accommodated in the finite element procedures.

L'article donne une description du genre d'éléments employés pour représenter des systèmes de sol-géotextiles afin de prédire leur fonctionnement en ce qui concerne contrainte et deformation. On donne les matrices de rigidité employées pour caractériser chacune de ces systèmes et l'on expose en détail les lois de contrainte et deformation qui ont été adoptées. Un montage d'éléments finis ainsi trouvé est appliqué ensuite à la prédiction du fonctionnement d'une fondation qui repose sur du sable compact avec ou sans une seule couche de géotextile placée a des profondeurs différentes en divers essais. Cela demontre que si les propriétés du sol sont representées d'une manière exacte dans les éléments du sol, une bonne correlation est obtenue entre les données prédites et les données mesurées, jusqu'à 85% environ de charge maximum. Au-dessus de cela, la méthode 'élément fini' est peu appropriée parce qu'il y a la possibilité d'echecs locaux du sol qui ne sont pas inclus dans les procédures 'élément fini'.

## INTRODUCTION

The behaviour of soil structures containing tension resistant inclusions such as geotextiles, depends not only on the properties of the soil and the inclusions but on the interaction of the soil and inclusions at interfaces. The success of any method of analysis for such a system will to a large extent be determined by its ability to represent these various material properties and interactions. At the present time, the finite element method approach involving discrete representation of the different constituents of the system offers a possible if somewhat complex method of analysis. Perhaps due to its complexity, few previous investigators have attempted to apply it to soil-geotextile systems (1, 2 and 3). In this paper, the work carried out at Strathclyde University, to develop a suitable finite element method approach for soil-geotextile systems which does allow such relative momement is described. Also its accuracy and limitations are identified by making comparisons between finite element method predictions and observations for laboratory scale prototypes of strip-footing loading systems.

## FINITE ELEMENT REPRESENTATION OF SOIL-GEOTEXTILE SYSTEMS

The finite element procedure used is basically that for solving continuum load-displacement problems, (4, 5 and 6). It consists of three main steps: the discretization of the continuum; the derivation of element stiffness matrices and the analysis of the element assemblage.

### Discretization of the Continuum:

In order to extend the finite element procedures for continuum problems to deal with soil-geotextile systems, particular types of elements have been developed to represent the soils, the geotextiles and the soil-geotextile interaction. These elements may be described as follows:

a) Soil elements: The soils are represented by triangular and quadrilateral elements, as shown in Fig. 1. The triangular elements are constant strain elements in which the displacement function is linear. The quadrilateral elements are considered to be formed from four triangular elements. Each triangular element stiffness is derived with two degrees of freedom allowed for any given point in the elements (6). The relationship between strains and small displacements is used (7) and the stiffness matrix is derived using the principle of minimum potential energy, which is a variational approach. The stiffness matrix may be given in the generalised form:

$$[Ke]\{\delta e\} = \{Pe\} \qquad .....(1)$$

where $[Ke]$ is the stiffness matrix of the elements, $\{\delta e\}$ is the vector of nodal displacements and $\{Pe\}$ is the vector of nodal forces.

The stiffnesses of the quadrilateral elements are derived by calculating the global stiffness of its four constituent triangular elements. By eliminating the degrees of freedom of the internal node of the quadrilateral elements, i.e. making use of a procedure called condensation (8), the stiffness matrices can be reduced to 8 x 8 matrix configurations without loss of accuracy.

b) Geotextile elements: The geotextiles are represented by straight line elements which have no bending stiffness and are of the form shown in Fig. 1. These elements can deform only in the axial direction and their displacement functions are linear (6). The stiffness matrix used is shown here in an incremental form:

$$\begin{Bmatrix} \Delta F_{x_1} \\ \Delta F_{y_1} \\ \Delta F_{x_2} \\ \Delta F_{y_2} \end{Bmatrix} = \frac{AE_t}{L} \begin{bmatrix} C^2 & SC & -C^2 & -SC \\ SC & S^2 & -SC & -S^2 \\ -C^2 & -SC & C^2 & -SC \\ SC & -S^2 & SC & S^2 \end{bmatrix} \begin{Bmatrix} \Delta U_1 \\ \Delta V_1 \\ \Delta U_2 \\ \Delta V_2 \end{Bmatrix} \quad \ldots\ldots(2)$$

which may be rewritten as:

$$\{\Delta F\} = [Ke]\ \{\Delta\delta\} \quad \ldots\ldots(3)$$

where $\{\Delta F\}$ is the vector of nodal force increments, $\{\Delta\delta e\}$ is the vector of nodal displacement increments and $[Ke]$ is the element stiffness matrix. Also $E_t$ is the element instantaneous elastic modulus, A is its cross sectional area and L its length. S is sin $\alpha$ and C is cos $\alpha$, where $\alpha$ is the inclination of the element to the x-axis.

c) Soil-geotextile interface elements: Soil-geotextile and soil boundary interactions are assumed to be purely frictional and simulated by spring elements of zero length connecting the nodes of soil elements to those of inclusion elements (9), as shown in Fig. 1, and its stiffness matrix may be written in incremental form as follows:

$$\begin{Bmatrix} \Delta F_{x_1} \\ \Delta F_{y_1} \\ \Delta F_{x_2} \\ \Delta F_{y_2} \end{Bmatrix} = \begin{bmatrix} K_hS^2+K_vC^2 & K_hSC-K_vSC & -K_hS^2-K_vC^2 & -K_hSC+K_vSC \\ & K_hC^2+K_vS^2 & -K_hSC+K_vSC & -K_hC^2-KS^2 \\ & & K_hS^2+K_vC^2 & K_hSC-K_vSC \\ & \text{(symmetrical)} & & K_hC^2+K_vS^2 \end{bmatrix} \begin{Bmatrix} \Delta U_1 \\ \Delta V_1 \\ \Delta U_2 \\ \Delta V_2 \end{Bmatrix} \quad \ldots\ldots(4)$$

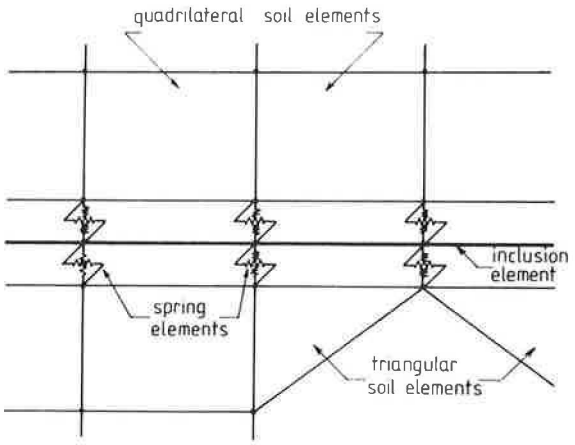


Fig. 1. Elements used in the analysis

which may be rewritten as:

$$\{\Delta F\} = [Ke]\ \{\Delta\delta e\} \quad \ldots\ldots(5)$$

where $\{\Delta F\}$ is the vector of nodal force increments, $\{\Delta\delta e\}$ is the vector of nodal displacement increments and $[Ke]$ is the element stiffness matrix. Also $K_h$ is the spring stiffness in the plane of the geotextile and $K_v$ is the spring stiffness perpendicular to it. Again S is sin $\alpha$ and C is cos $\alpha$ where $\alpha$ is the inclination of the element to the x-axis.

From a comparison of equations (2) and (4), it can be seen that the spring element stiffness can be constructed by superimposing the stiffness matrices of two line elements, one parallel to the inclusion and the other perpendicular to it. During the analysis, the spring element is permitted to elongate, or compress, but only in the direction parallel to the geotextile plane. This allows the development of relative sliding between the soil and the geotextile. Relative movement perpendicular to the geotextile is restricted by assigning a very large stiffness ($K_v$) to the spring element in this direction.

Derivation of Element Stiffness

To obtain the stiffness of each element the stress-strain behaviour of the various components and interfaces must be represented in mathematical form. To do this different mathematical techniques were adopted for the soils, the inclusions and their interfaces. Taking them in turn:

a) Stress-strain model of soil behaviour: To represent the soil, the non-linear elastic hyperbolic model is used (10, 11). It is also assumed that the initial tangent modulus ($E_i$) is related to the confining pressure ($\sigma_3$) as follows:

$$E_i = KPa\left(\frac{\sigma_3}{Pa}\right)^n \quad \ldots\ldots(6)$$

where Pa is atmospheric pressure, K and n are dimensionless constants, (12).

Thus the instantaneous tangent modulus can be expressed as

$$E_t = \left[1 - \frac{R_f\ (1 - \sin\phi)(\sigma_1 - \sigma_3)}{(2c\cos\phi + 2\sigma_3\sin\phi)}\right]^2 KPa\ \left(\frac{\sigma_3}{Pa}\right)^n \ldots(7)$$

where $R_f$ is the ratio of deviator stress in the soil at failure to the ultimate deviator stress, c is the soil cohesion and $\phi$ is the angle of soil friction.

To include the effect of the curvature of the Mohr failure envelope in cohesionless soils, the following is added:

$$\phi = \phi_0 + \Delta\phi\ \log_{10}\left(\sigma_3/Pa\right) \quad \ldots\ldots(8)$$

where $\phi_0$ is the value of $\phi$ for $\sigma_3$ equal to atmospheric pressure Pa, and $\Delta\phi$ is a material constant equal to the reduction in $\phi$ for a 10 fold increase in $\sigma_3$, (13).

The above equations provide all the information required for the evaluation of the instantaneous tangent modulus at any stress level and any confining stress during the incremental finite element analysis. To obtain the instantaneous Poisson's ratio, the expression used was:

$$\mu_t = \frac{G - F\log\left(\sigma_3/Pa\right)}{\left[1 - \dfrac{d(\sigma_1 - \sigma_3)}{KPa\left(\frac{\sigma_3}{Pa}\right)^n\left[1 - \dfrac{R_f(1 - \sin\phi)(\sigma_1 - \sigma_3)}{2c\cos\phi + 2\sigma_3\sin\phi}\right]}\right]^2} \quad \ldots(9)$$

where G equals the value of initial Poisson's ratio $\mu_i$

at one atmosphere, F equals the reduction in $\mu_i$ for a ten fold increase in $\sigma_3$ and d is a constant.

The value of Poisson's ratio cannot exceed 0.5 as it will violate the condition of positive strain energy, hence, volume expansion is not taken into account in this analysis. Also a Poisson's ratio of 0.5 cannot be used as it would lead to an infinite bulk modulus. To overcome this, when a value of 0.5 or more is encountered, a value of 0.49 is assigned to the element. To relate the stresses and strains in the soil, the incremental stress-strain equation proposed is:

$$\begin{Bmatrix} \Delta\sigma_x \\ \Delta\sigma_y \\ \Delta\tau_{xy} \end{Bmatrix} = \begin{bmatrix} Mb + Md & Mb - Md & 0 \\ Mb - Md & Mb + Md & 0 \\ 0 & 0 & Md \end{bmatrix} \begin{Bmatrix} \Delta\varepsilon_x \\ \Delta\varepsilon_y \\ \Delta\gamma_{xy} \end{Bmatrix} \quad .....(10)$$

where $\Delta\sigma_x$ and $\Delta\sigma_y$ are the incremental stresses in the x and y directions respectively and $\Delta\tau_{xy}$ is the incremental shear stress. $\Delta\varepsilon_x$ and $\Delta\varepsilon_y$ are the incremental strains in the x and y directions respectively and $\Delta\gamma_{xy}$ is the incremental shear strain (14).

Also Md is the instantaneous shear modulus and

$$Md = \frac{E_t}{2(1 + \mu_t)} \quad .....(11)$$

with Mb the instantaneous bulk compressibility and

$$Mb = \frac{E_t}{2(1 + \mu_t)(1 - 2\mu_t)} \quad .....(12)$$

These moduli are used assuming Mb is a constant for a given confining pressure $\sigma_3$, but varies with $\sigma_3$ according to the corresponding initial tangent modulus $E_i$ and initial Poisson's ratio $\mu_i$ (15). Thus Mb is calculated as follows:

$$Mb = \frac{E_i}{2(1 + \mu_i)(1 - 2\mu_i)} \quad .....(13)$$

With the above equations then the stiffness matrices for the soil elements may be evaluated.

b) Stress-strain model of geotextile behaviour: As the load extension relationships for geotextiles are usually non-linear, they cannot be accurately simulated by linear relationships. Polynomial functions have therefore to be used and the function that is chosen has the form:

$$T = A\sigma = a_1\varepsilon + a_2\varepsilon^2 + a_3\varepsilon^3 ... \quad .....(14)$$

where T is the axial load applied to the geotextile, A is the initial cross sectional area, $\sigma$ is the "apparent axial stress", calculated by assuming the geotextile does not change its cross-sectional area during axial straining, $\varepsilon$ is the axial strain and $a_1$, $a_2$, $a_3$... are polynomial constants.

By differentiating equation (14) with respect to $\varepsilon$, the product of the instantaneous tangent modulus $E_t$ and the initial cross sectional area A, can be directly evaluated from strains as follows:

$$\frac{dT}{d\varepsilon} = \frac{d(A\sigma)}{d\varepsilon} = \frac{Ad\sigma}{d\varepsilon} = AE_t = a_1 + 2a_2\varepsilon + 3a_3\varepsilon^2 \quad ...(15)$$

The product $AE_t$ is then used directly to evaluate the stiffness matrices of the geotextile elements as indicated in equation (2). The constants $a_1$, $a_2$, $a_3$... are determined by the least square curve fitting technique of measured load-extension curves (16)

c) Shear stress-deformation model of soil-geotextile interface friction: A hyperbolic model is adopted to simulate the interface friction behaviour of soil-geotextile and soil in contact with boundaries. The model used is as follows:

$$\tau = \frac{\delta r}{b_1 + b_2\delta r} \quad .....(16)$$

where $\tau$ is the shear stress and $\delta r$ is the relative displacement at the interface for a given normal stress $\sigma_n$ (15). Also $b_1$ and $b_2$ are constants equal to $(1/k_i)$ and $(1/\tau_{ult})$ respectively, where $k_i$ is the initial tangent stiffness per unit area and $\tau_{ult}$ is the asymptotic value of the shear stress at infinite displacement of the hyperbolic curve. The initial tangent stiffness per unit area ($k_i$) is assumed to be related to the normal stress ($\sigma_n$) by the following expression:

$$k_i = K_1 Pa\left(\frac{\sigma_n}{Pa}\right)^{n_1} \quad .....(17)$$

where $K_1$ and $n_1$ are constants.

In a manner similar to that for the instantaneous tangent modulus of soil, the instantaneous tangent stiffness of the interface can be expressed as

$$k_t = \left[1 - \frac{Rf_1\tau}{\sigma_n \tan\delta}\right]^2 K_1 Pa\left(\frac{\sigma_n}{Pa}\right)^{n_1} \quad .....(18)$$

where $Rf_1$ is the ratio of the shear stress at failure to the ultimate shear stress on the interface and $\delta$ is the angle of friction between the soil and the geotextile. The instantaneous stiffness of the spring element ($K_t$) then becomes:

$$K_t = k_t - A \quad .....(19)$$

where A is the field area of the element.

## Analysis of the Element Assemblage

After evaluating the stiffness matrices for the individual elements, the stiffness matrix for the whole system is assembled. The basis of the assembly is that the value of the displacement at a node is the same for each element sharing the node (5). The assembly process results in a set of simultaneous equations of the same form as the equations for the individual elements, as follows:

$$[K_g]\{\delta\} = \{P\} \quad .....(20)$$

where $[K_g]$ is the global stiffness matrix, $\{\delta\}$ is the vector of all the nodal displacements and $\{P\}$ is the vector of the nodal forces.

The next step is to modify equation (20) to account for boundary conditions which may include zero or non-zero displacements. This is followed by the solution of the simultaneous equations for the unknown displacements. Finally, from the now known nodal displacements, the strains and stresses for each element are calculated to yield the complete solution.

In its present form the program can only deal with systems in which the initial stresses are either known or are calculated from the at-rest condition. Increments of load are then applied and the instantaneous tangent moduli for each increment of load are evaluated according to the position reached on the stress-strain curve. This is achieved using a two stage load cycle technique based on the mid-point integration method, (5).

## SYSTEMS AND MATERIALS MODELLED

Several soil-geotextile systems have now been modelled at Strathclyde University using the finite element procedure including the prediction of the measured behaviour of laboratory scale embankments (3). In these embankments the deformations and stresses in the system were relatively small and good correlation between measured and predicted behaviours were obtained.

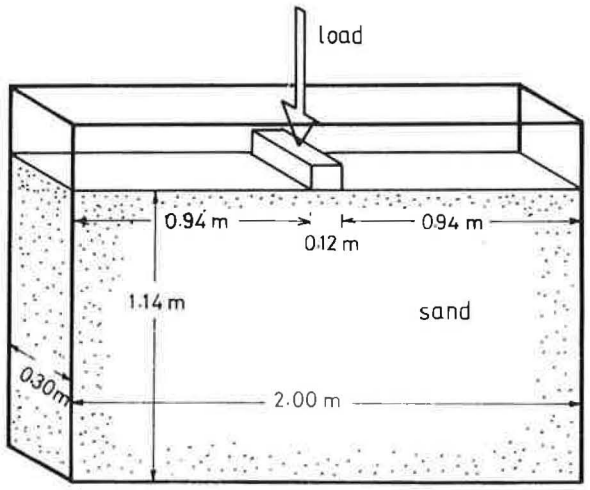


Fig. 2. Layout of apparatus

In this paper, comparisons are made between measured and predicted behaviour of laboratory scale soil-geotextile strip-footing loading tests which have been taken to failure and therefore involve large deformations and stresses. Prior to making these comparisons the nature of the system tested and the materials used are described.

System Tested:

The strip-footing tests were conducted in a large tank with 12.5 mm thick glass sides within a rigid steel frame. The principal dimensions and layout of the apparatus are shown in Fig. 2. The strip-footing used was 120 mm wide and made of rigid smooth steel plates. The load was applied to the footing by means of a motorised 10 tonne capacity screw jack at a constant rate of 0 mm per hour.

The sand used in both tests was Leighton Buzzard sand which is a sub-rounded, mainly quartzite sand with a particle size range of 0.3 - 2.0 mm and mean diameter of 0.85 mm. The uniformity coefficient was 1.22. It was placed in a dense state with a porosity of 34 per cent by an air activated spreader (17). The soil was tested under drained triaxial test conditions and the values of the hyperbolic parameters determined from these tests are shown in Table 1.

TABLE 1. HYPERBOLIC PARAMETERS FOR LEIGHTON BUZZARD SAND

| Parameters derived from triaxial tests | | | | | | | | | |
|---|---|---|---|---|---|---|---|---|---|
| K | $K_{ur}$ | n | c | $\phi_o$ | $\phi$ | $R_f$ | G | F | d |
| 1573 | 1890 | 1.05 | 0 | 42.7° | 3.2° | 0.9 | 0.46 | 0.17 | 24 |
| Parameters assumed and used in analysing the strip footing model tests | | | | | | | | | |
| K | $K_{ur}$ | n | c | $\phi_o$ | $\phi$ | $R_f$ | G | F | d |
| 1573 | 1890 | 1.05 | 0 | 49° | 0 | 0.9 | 0.45 | 0 | 0 |

The geotextile used as the inclusion was a non-woven melt-bonded material made from 67 per cent polypropylene and 33 per cent polyethylene, manufactured by ICI Fibres and known as "Terram 1000". It possessed a mass per unit area of 140 g/m$^2$ and average thickness of 0.7 mm. The load-extension properties of the geotextile were established in the in-soil test apparatus (18). In the strain range and normal confining stress range applied in these tests, it was considered that a single average curve could be used to describe the load deformation behaviour of the geotextile. The polynomial coefficients used to model the curve are as shown in Table II.

TABLE II. POLYNOMIAL COEFFICIENTS FOR TERRAM 1000

| $a_1$ | $a_2$ | $a_3$ | $a_4$ | $a_5$ |
|---|---|---|---|---|
| 76.4 | -1347.4 | 20804 | -187422 | 982038 |
| $a_6$ | $a_7$ | $a_8$ | $a_9$ | $a_{10}$ |
| -2965793 | 47181650 | -3183505 | 0 | 0 |

Shear box tests were carried out to determine the interface properties between the geotextile and the sand and the footing and the sand. In these the geotextile and the steel and the footings were placed in the bottom half of the shear box level with the plane of sliding with the top half. The top half was filled with dense sand at a porosity of 34 per cent. The parameters obtained from these tests which were used in the analysis are given in Table III.

TABLE III. HYPERBOLIC PARAMETERS FOR INTERFACE FRICTION

| Leighton Buzzard sand in contact with Terram 1000 | | | |
|---|---|---|---|
| $K_1$ | $n_1$ | $R_{f_1}$ | $\delta$ |
| 1300 | 0.30 | 0.8 | 36.3° |
| Leighton Buzzard sand in contact with footing base | | | |
| $K_1$ | $n_1$ | $R_{f_1}$ | $\delta$ |
| 800 | 0.05 | 0.49 | 11.3° |

PREDICTED AND MEASURED STRIP FOOTING LOADS

Sand Alone:

To prove the reproducibility of test data from the apparatus, two tests were carried out on the footing placed on sand alone. As can be seen in Fig. 3 in dimensionless form, the load settlement relationship for these tests is typical of that for a strip footing resting on dense sand and shows very little variation between tests. Back analysis of the peak bearing pressures using classical bearing capacity theories suggests that the operational angle of friction for the sand lies between 48° and 50°. Now the level of stressing of the soil is much greater in these tests than it was in the embankment model tests previously reported (3), thus side friction in the apparatus is bound to be much greater. This would lead to an apparently higher value of the operational angle of friction. Also, at strain levels in the sand approaching peak stresses, the differences between the behaviour in plane strain and triaxial test conditions becomes more marked than at low strain levels. In fact it has been suggested that the angle of friction to be used in plane strain bearing capacity calculations should be 10 per cent higher than that measured in triaxial tests in order to account for this, (19, 20). A combination of these factors could therefore well explain the average 12 per cent difference between measured triaxial values and the back analysed values from footing test data.

The finite element mesh used to model the strip footing on sand alone consisted of 285 rectangular soil elements each formed of four constant strain triangular elements with, on this occasion, only 5 spring elements

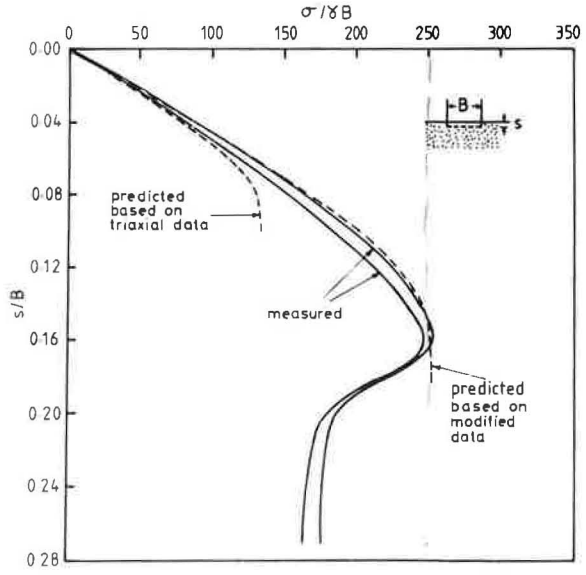


Fig. 3. Sand alone - bearing pressure vs settlement (dimensionless)

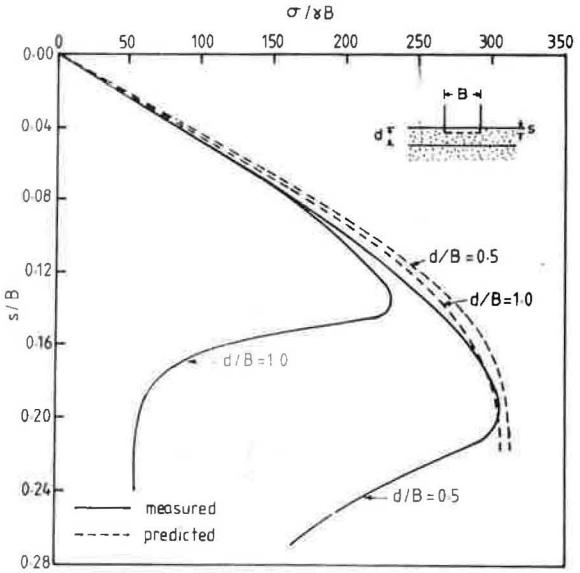


Fig. 4. Sand with inclusion - bearing pressure vs settlement (dimensionless).

used to represent the soil-footing interface. The loading was applied in steps which corresponded to a constant displacement increment of 1 mm. Geometrical changes of the elements during strain were ignored.

Using the parameters indicated in Tables I, II and II, the predicted load settlement relationships for the strip footing resting on the sand were as shown in Fig. 3. This indicates a peak footing stress approximately half that measured although the initial load settlement relationship is in reasonably good agreement. This indicates that the value of angle of friction used for the sand is most probably the parameter in error. To overcome this and to simplify the analysis somewhat, it was decided to adopt a constant value for the angle of friction of the sand equal to the average back analysed test data value of 49°. Also to provide less erratic patterns of stresses beneath the footing, a constant Poisson's ratio value of 0.45 was adopted. With these changes, the predicted load-settlement curve became much more accurate, as shown in Fig. 3, although it did not indicate the measured reduction in bearing capacity at post peak strains. This is to be expected as strain softening is not included in the finite element analysis.

Sand with a Single Geotextile Inclusion Layer:

Tests were conducted on the strip-footing resting on sand containing a single layer of geotextile placed at different depths as it was known from small scale tests that the depth of the geotextile was an important factor, (21). Predictions were made of the behaviour of these systems using the finite element procedure. The mesh used was the same as for the sand alone but with the addition of 14 line elements to represent the geotextile and 30 spring elements to represent the soil-geotextile interfaces. The reorientation of the line elements during straining was allowed for. The parameters used to model the materials and their interfaces were the modified parameters used for the tests on soil alone.

The measured and predicted data for two cases are given in Fig. 4. They show that for the case where the geotextile was placed at a depth equal to half the breadth of the footing (0.5 B), the measured and predicted behaviours were within 10 per cent up to peak footing load. For the case where the footing was placed at a depth equal to the breadth of the footing (1.0 B), the measured and predicted behaviours were again within 10 per cent but only up to 85 per cent of the measured peak load. Beyond this, the predicted behaviour rapidly diverges from the measured behaviour and grossly overestimates the bearing capacity of the footing. Examination of the strain fields obtained from measured displacement data shows that sliding along the geotextile occurred in this test at strains approaching peak loads and that locally the soil above and in close proximity to the geotextile was subject to large strains. Thus post peak strain softening was probably occurring in this region and this is not allowed for in the finite element analysis.

It is very interesting to note from the measured and predicted data that the influence of the geotextile on the load-settlement behaviour of the strip footing was very limited up to settlements equal to approximately 8 per cent of the footing breadth. This suggests that up to that level of settlement, strains in the soil were insufficient to mobilise significant tensile load in the geotextile.

DISCUSSION

The finite element method of analysis involving discrete representation of the different constituents within soil-geotextile systems has been described in this paper and shown to be a valuable analytical method. It has been found to be limited to the analysis of the behaviour of soil-geotextile systems prior to failure developing in any of their constituent materials, even locally. Whenever such a failure developed, the predicted behaviour was found to rapidly diverge from the actual behaviour since the mathematical laws used in the analysis to represent the stress-strain behaviour of the constituents do not allow for any strain softening that occurs. The finite element procedure does, nevertheless, provide up to this failure stage, a good prediction of system behaviour.

The principal difficulty of representing the materials behaviour is with the soil. It appears from the work so far undertaken that triaxial test data can underestimate the strength of soils in plane strain. Thus in the analysis reported in this paper it was found necessary to increase the value used in the analysis by 8 to 10 per cent over that from triaxial tests to allow for this. A further 4 to 2 per cent was added to allow for side friction in the plane strain test apparatus, to give an average overall increase of 12 per cent.

Although the finite element procedure described in this paper is limited to pre-failure conditions, these are likely to be appropriate to the range of operational stress and strains in many soil-geotextile systems. Thus this method is likely to be a valuable means of testing the significance of varying different soil and geotextile properties. Also it will allow the significance of varying construction procedures to be established. Much development is still required for this finite element procedure but the results so far obtained suggest that it will be worthwhile pursuing this analytical method.

ACKNOWLEDGEMENTS

The authors gratefully acknowledge the financial support given to this work by ICI Fibres and the Egyptian Government.

REFERENCES

(1) Bell, J. R., Greenway, D. R. and Vischer, W. "Construction and Analysis of a Fabric Reinforced Low Embankment on Muskeg," Proceedings of International Conference on Use of Fabrics in Geotechnics, (Paris, 1977), Vol 1, 71-76.

(2) Mashhour, M. M., The Behaviour of Model Granular Embankments With and Without Fabric Inclusions. PhD Thesis, (University of Strathclyde, 1979).

(3) Andrawes, K. Z., McGown, A., Mashhour, M. M. and Wilson-Fahmy, R. F., "Tension Resistant Inclusions in Soils," Journal Geotechnical Engineering Division, ASCE, 106 (1980), 1313-1326.

(4) Zienkiewicz, O. C., Finite Element Method in Engineering Science, McGraw-Hill, (New York, 1971).

(5) Desai, C. S. and Abel, J. F., Introduction to the Finite Element Method, Van Nostrand-Reinhold Co., (New York, 1972).

(6) Huebner, K. H., The Finite Element Method for Engineers, Wiley and Sons, (New York, 1975).

(7) Love, A. E. H., A Treatise on the Mathematical Theory of Elasticity, Dover Publications, (New York, 1944).

(8) Fellipa, C. A. and Clough, R. W., "The Finite Element Method in Solid Mechanics," Proceedings Numerical Solutions of Field Problems in Continuum Physics SIAM-AMS, (1970), American Mathematical Society, 2.

(9) Ngo, D. and Scordelis, A. C., "Finite Element Analysis of Reinforced Concrete Beams," ACI Journal, 63 (1967), Vol 3 152-162.

(10) Duncan, J. M. and Chang, C. Y., "Non-linear Analysis of Stress and Strain in Soils," Journal Soil Mechanics and Foundation Engineering Division, ASCE, 96, (1970), SM5, 1629-1653.

(11) Kulwahy, F. H. and Duncan, J. M., "Stresses and Movements in Oroville Dam," Journal Soil Mechanics and Foundation Engineering Division, ASCE, 98, (1972), SM7, 653-655.

(12) Janbu, N., "Soil Compressibility as Determined by Oedometer and Triaxial Tests," Proceedings of European Conference on Soil Mechanics and Foundation Engineering, (Wiesbaden, 1963), Vol 1, 19-25.

(13) Wong, K. S. and Duncan, J. M., "Hyperbolic Stress-Strain Parameters for Non-Linear Finite Element Analysis of Stresses and Movements in Soil Masses," Report No TE 74.3, Department of Civil Engineering, University of California, (Berkeley, 1974), 90 pp.

(14) Clough, R. W. and Woodward, R. J. "Analysis of Embankment Stresses and Deformations," Journal Soil Mechanics and Foundation Engineering Division, ASCE, 93, (1967), 529-549.

(15) Clough, G. W. and Duncan, J. M., "Finite Element Analysis of Retaining Wall Behaviour," Journal Soil Mechanics and Foundations Division, ASCE, 97, (1971), SM12, 1657-1673.

(16) Hornbeck, R. W., Numerical Methods, Quantum Pub. Inc. (1975).

(17) Butterfield, R. and Andrawes, K. Z., "An Air Activated Sand Spreader for Forming Uniform Sand Beds," Geotechnique, (1970), Vol 20, 97-100.

(18) McGown, A., Andrawes, K. Z., Wilson-Fahmy, R. F. and Brady, K. C., "A New Method of Determining the Load Extension Properties of Geotechnical Fabrics," Department of Environment, Department of Transport, TRRL Report SR 704, (1981), 14 pp.

(19) Meyerhof, G. G., "Discussion." Proceedings of Fifth International Conference on Soil Mechanics and Foundation Engineering, (1965), Vol 3, 193-194.

(20) Hansen, J. B., "A Revised and Extended Formula for Bearing Capacity," Danish Geotechnical Institute Bulletin, (1970), Vol 28, 5-11.

(21) McGown, A. and Andrawes, K. Z., "The Influence of Non-Woven Fabric Inclusions on the Stress-Strain Behaviour of a Soil Mass," Proceedings of International Conference on Use of Fabrics in Geotechnics, (Paris, 1977), Vol 1, 161-166.

Wieder der Hinweis auf Unterschätzung der Erdwiderstandswerte infolge Triaxialversuch bei dem Verformungsrichtungen behindert ist dgl. nicht ⇒ Foundations 2(

Widerspruch?